Title page

Exosomal miR-224 contributes to hemolymph microbiota homeostasis during bacterial infection in crustacean

Yi Gong[1,2,3], Xiaoyuan Wei[1,3], Wanwei Sun[1,3], Xin Ren[1,3], Jiao Chen[1,3], Jude Juventus Aweya[1, 2,3], Hongyu Ma[1,2,3], Kok-Gan Chan[3,4], Yueling Zhang[1,2,3*], Shengkang Li[1,2,3*]

[1]*Guangdong Provincial Key Laboratory of Marine Biology, Shantou University, Shantou 515063, China*

[2]*Southern Marine Science and Engineering Guangdong Laboratory, Guangzhou, China*

[3]*Institute of Marine Sciences, Shantou University, Shantou 515063, China*

[4]*Division of Genetics and Molecular Biology, Institute of Biological Science, Faculty of Science, University of Malaya, 50603 Kuala Lumpur, Malaysia*

* Corresponding author: Yueling Zhang; Shengkang Li

Tel: +86-754-86502485

Fax: +86-754-86503473

Email: lisk@stu.edu.cn

Abstract

The modulation of hemolymph microbiota homeostasis is vital for the marine invertebrate innate immunity, while growing evidence shows that exosomes could serves as anti-bacterial immune factors, however, the relationship between exosomes and hemolymph microbiota homeostasis during pathogenic bacteria infection has not been addressed. Here, we determined that exosomes released from *Vibrio parahaemolyticus*-infected *Scylla paramamosain* (mud crabs) could reduce the mortality of the host during the infection by maintaining the homeostasis of hemolymph microbiota. We further confirmed that miR-224 was densely packaged in these exosomes and targeting to HSP70, which resulted in disruption of the HSP70-TRAF6 complex to release TRAF6 that allows it to interact with Ecsit. The interaction of TRAF6 with Ecsit regulates the production of mitochondrial ROS (mROS) and Anti-lipopolysaccharide factors (ALFs) expression in recipient hemocytes, which affects homeostasis of hemolymph microbiota in response to the pathogenic bacteria infection in mud crab. To the best of our knowledge, this is the first document that reports the role of exosome in the homeostasis of hemolymph microbiota during pathogen infection and a novel regulatory mechanism and crosstalk between exosomal miRNAs and innate immune response in crustaceans.

Keywords: *Scylla paramamosain*; *Vibrio parahaemolyticus*; hemolymph microbiota; exosomal miR-224; HSP70; TRAF6-Ecsit complex

Author summary

Exosomes are small membrane vesicles of endocytic origin which are widely involved in the regulation of a variety of pathological processes in mammals. Yet, although the antibacterial function of exosomes has been discovered for many years, the relationship between exosomes and hemolymph microbiota homeostasis remains unknown. In the present study, we identified the miRNAs packaged by exosomes that were possibly involved in *Vibrio parahaemolyticus* infection by modulating hemolymph microbiota homeostasis in crustacean mud crab *Scylla paramamosain*. Moreover, it was found that miR-224 was densely packaged in exosomes after *Vibrio parahaemolyticus* challenge, resulting in the suppression of HSP70 and disruption of the HSP70-TRAF6 complex in recipient hemocytes, then the released TRAF6 was further interacted with Ecsit to regulate ROS and ALFs levels, which eventually affected hemolymph microbiota homeostasis to cope with pathogenic bacteria infection. Our finding is the first to reveal the relationship between exosomes and hemolymph microbiota homeostasis in animals, which shows a novel molecular mechanism of invertebrate resistance to pathogenic microbial infection.

Introduction

Exosomes are microvesicles (measuring 30-120 nm in diameter) formed in multivesicular bodies and released into the extracellular environment under physiological and pathological conditions (Colombo et al., 2014; Tkach and Théry, 2016). Specific proteins highly enriched in exosomes such as TSG101, CD63 CD81 and flotillin 1, are usually served as markers for the identification of exosomes (Bobrie et al., 2012). Exosomes can be secreted by various donor cells and transferred to target cells by fusing with cytomembranes, which serve as mediators during intercellular communications via transporting bio-cargoes, such as nucleic acids, proteins and lipids (Milane et al., 2015; Valadi et al., 2007). Given their role as a form of intercellular vesicular transport, numerous studies have pointed out the importance of exosomes during pathogen infection and immune response (Marta and Maria, 2015; Wang et al., 2014b). It is believed that pathogen-infected cells are capable of secreting exosomes that contain pathogens or host genetic elements to neighboring cells to help modulate host immune response, which has huge impact on the fate of the infection process (Hammond et al., 2000; Marisa and Chioma, 2015). However, very little is known about how exosomes regulate host immune response and impact on pathogen infection, especially in crustaceans.

MicroRNAs (miRNAs), a class of small non-coding RNAs with 18-25 nucleotides in length, can interact with the complementary sequences on the 3' untranslated region (3'UTR) of target mRNA to either arrest translation or degrade the mRNA of the target genes (Ambros, 2004; Schroeder, 2007). Apart from their endogenous functions, miRNAs can be packaged into exosomes to modulate the expression of specific target genes in recipient cells (Bang et al., 2014; Fong et al., 2015). Furthermore, recent studies have revealed that loading of miRNAs into exosomes is a selective process and

can reflect the dysregulated miRNA composition in donor cells (Mario et al., 2014). It has been demonstrated that alteration of exosomal miRNA composition has great influence on the biological activities of exosomes that have been taken-up during pathogens infection (Gurwitz, 2015; Zhang et al., 2015). Importantly, RNA sequencing analysis reveals that miRNAs are the most abundant RNA species in exosomes, accounting for more than 40% (Boorn et al., 2013). It is thought that exosome-mediated intercellular transfer of miRNAs can regulate pathogens spread and immune defense in recipient cells, which suggest that exosomal miRNAs could play potential role as novel tools for intercellular communication.

Crustaceans have an open circulatory system, where hemocytes, oxygen, hormones and nutrients circulate together in the hemolymph (Söderhäll, 2016). Symbiotic microorganisms are indispensable inhabitants in the host (Douglas, 2018), with growing evidence showing the presence of diverse microorganisms in the hemolymph of aquatic invertebrates including shrimp (Wang and Wang, 2015), scallop (Lokmer and Mathias, 2015) and crab (Tubiash et al., 1975). Generally, the proliferation of microbiota in the nutrient rich hemolymph environment is tightly controlled by host immune factors such agglutination, phagocytosis, production of antimicrobial peptides and reactive oxygen species (ROS) (Sun et al., 2017; Wang and Wang, 2015). For instance, it has been shown that a shrimp C-type lectin, *Mj*HeCL, maintains hemolymph microbiota homeostasis by modulating the expression of antimicrobial peptides (Wang et al., 2014a). Hemolymph symbiotic microbiota in hemolymph are believed to be engaged in multiple functions in the host, including competing with invading pathogens or stimulating the host to mount an immune response during pathogens infection (Florie et al., 2014; Paulina et al., 2012). Unfortunately, uncontrol proliferation of hemolymph microbiota could result in host

diseases such as “Milky Disease” or “Early Mortality” (Li et al., 2012; Zhang et al., 2018), which highlights the importance of hemolymph microbiota in host immune system and disease prevention.

Our unpublished study revealed that during infection of *Scylla paramamosain* (mud crab) with *V. parahaemolyticus*, there was a significant change in the diversity and abundance of hemolymph microbiota, which are vital indicators of health status. It would therefore be important to explore the relevant molecular mechanisms involved in the modulation of host hemolymph microbiota homeostasis during infection by pathogens. The open circulatory system of crustaceans makes it an ideal carrier for exosomes to perform immune-related functions. However, the role of exosomes in maintaining hemolymph microbiota homeostasis remains unclear. In the light of this, the current study explored the relationship between exosomes and hemolymph microbiota in mud crab. Exosomes released from *Vibrio parahaemolyticus*-infected mud crabs could reduce crab mortality due to *V. parahaemolyticus* infection by maintaining the homeostasis of hemolymph microbiota. Moreover, miR-224 was found to accumulate in exosomes after *V. parahaemolyticus* infection, which resulted in suppression of HSP70 (Heat shock protein 70) and disruption of the HSP70-TRAF6 (TNF receptor associated factor 6) complex. The released TRAF6 then interacted with Ecsit (Evolutionarily conserved signaling intermediate in Toll pathways) to regulate mROS (mitochondrial ROS) production and the expression of ALFs (Anti-lipopolysaccharide factors) in the recipient hemocytes, which eventually affected hemolymph microbiota homeostasis in response to the infection.

Results

The involvement of exosomes in anti-bacterial response in mud crab

136 To explore the involvement of exosomes from mud crab in bacterial infection,
137 exosomes isolated from the hemolymph of *V. parahaemolyticus*-challenged mud crabs
138 (i.e., exosome-Vp) and PBS (Phosphate buffer saline)-injected control crabs (i.e.,
139 exosome-PBS). The typical cup-shaped structures of isolated exosomes were observed
140 under an electron microscope (Fig. 1A) and their sizes measured by Nanosight particle
141 tracking analysis (Fig. 1B). The isolated particles were further ascertained as exosomes
142 by determining the exosomal protein markers Flotillin-1, TSG101 and the cytoplasmic
143 marker Calnexin using Western blot analysis (Fig. 1C). These results indicate
144 successful isolation of exosomes from mud crabs challenged with *V. parahaemolyticus*
145 and PBS.

146 Next, the ability of the isolated exosomes to be internalized by mud crab
147 hemocytes was analyzed by labeling the isolated exosomes with DiO (green) before
148 being injected into mud crabs. When hemocytes from the injected crabs were collected
149 and labeled with DiI (red) before being examined with a confocal laser scanning
150 microscope, the results showed that the isolated exosomes could be internalized in
151 hemocytes (Fig. 1D). To explore the involvement of exosomes in mud crab during
152 pathogenic bacteria infection, the isolated exosomes (exosome-Vp and exosome-PBS)
153 were mixed with *V. parahaemolyticus* or PBS (control) before being injected into mud
154 crabs to determine the mortality rate. As shown in Fig. 1E, there was significant
155 reduction in the mortality rate of mud crabs injected with exosome-Vp mixed with *V.*
156 *parahaemolyticus* compared with mud crabs injected with exosome-PBS mixed with
157 *V. parahaemolyticus*, which suggest that exosomes isolated from *V. parahaemolyticus*-
158 challenged mud crabs have an effect on pathogenic bacteria infection and therefore
159 affecting the mud crab mortality rate. Moreover, when the relative abundance of
160 hemolymph bacteria in mud crabs was determined, the results revealed that exosome-

Vp was able to inhibit the rapid increase in hemolymph bacteria during infection (Fig. 1F). Taken together, these results suggest that exosomes secreted by *V. parahaemolyticus*-challenged mud crabs play a role in anti-bacterial response in mud crabs, probably by helping to maintain homeostasis of hemolymph microbiota.

Exosomes modulate hemolymph microbiota homeostasis

To ascertain the regulatory function of exosomes in modulating the mud crab hemolymph microbiota homeostasis, we determined the expression of antimicrobial peptides (AMPs) and ROS level, which are essential in regulating hemolymph microbiota homeostasis (Sun et al., 2017; Wang and Wang, 2015). The results revealed that exosome-Vp treatment could significantly increase ROS levels in mud crabs during pathogenic bacteria infection compared with the exosome-PBS (Figs. 2A and 2B). Similarly, transcript levels of ALF1, ALF4 and ALF5 were significantly increased in mud crabs treated with exosome-Vp (Fig. 2C). Next, the bacteria species and composition of hemolymph microbiota were analyzed using 16S rDNA sequencing. As shown in Fig. 2D, the diversity of hemolymph microbiota in mud crabs decreased significantly during *V. parahaemolyticus* infection. However, hemolymph microbiota diversity was maintained during the infection following treatment of mud crabs with exosome-Vp as compared with exosome-PBS. When the composition of hemolymph microbiota was analyzed at the phylum level, the proportion of *Proteobacteria*, *Tenericutes* and *Firmicutes* increased during *V. parahaemolyticus* infection, while the proportion of *Acidobacteria*, *Actinobacteria* and *Chloroflexi* decreased. On the contrary, when mud crabs were treated with exosome-Vp, microbiota homeostasis was maintained in mud crabs during the infection (Fig. 2E). A similar trend was observed when the top 35 genera of hemolymph microbiota was analyzed (Fig. 2F), which is in agreement with our data found in *V. parahaemolyticus*-resistant crabs collected from

the field (unpublished results). All these results suggest that during pathogenic bacteria infections in mud crabs, exosomes modulate pathways that maintain the homeostasis of hemolymph microbiota by regulating the levels of mROS and ALFs.

Functional miRNA screening in exosomes

To determine the functional exosomal miRNAs that are crucial in modulating hemolymph microbiota homeostasis, miRNA microarray analysis was carried out using exosome-Vp and exosome-PBS treated mud crab samples. Among the differentially expressed miRNAs, the top 6 miRNAs (Fig. 3A) which include miR-291, miR-343, miR-224, miR-189, miR-60 and miR-156 were selected to investigate their role in *V. parahaemolyticus* infection in mud crabs. The miRNA mimics and anti-miRNA oligonucleotides (AMOs) of these miRNAs were synthesized and co-injected with *V. parahaemolyticus* into mud crabs followed by qPCR analysis of ALF1 expression. The results revealed that injection of mud crabs with miR-224 mimics increased the expression of ALF1, while injection with AMO-miR-224 decreased the ALF1 expression (Figs. 3B and 3C).

To ascertain whether exosome-Vp was involved in regulating hemolymph microbiota homeostasis via miR-224, the relative expression level of miR-224 was determined in exosome-Vp and exosome-PBS injected mud crabs. The results revealed significant upregulation in the expression of miR-224 in the exosome-Vp injected mud crabs compared with exosome-PBS (Fig. 3D). Next, the involvement of miR-224 in the exosome-mediated regulatory process was examined by co-injecting *V. parahaemolyticus* with exosome-PBS, exosome-Vp or exosome-Vp and AMO-miR-224 into the mud crabs. The level of ROS in the exosome-Vp and AMO-miR-224 co-injected mud crabs was significantly lower compared with the other mud crabs (Fig. 3E and 3F). A similarly trend was observed in the expression levels of ALF1, ALF4 and

ALF5 for these mud crab samples (Fig. 3G). In addition, 16S rDNA sequencing analysis revealed a disruption in the exosome-Vp-mediated hemolymph microbiota homeostasis upon miR-224 silencing (Fig. 3H and 3I). These results suggest that miR-224 is controlled by *V. parahaemolyticus*-derived exosomes to maintain hemolymph microbiota homeostasis in mud crabs.

Interactions between miR-224 and its target gene

To explore the pathways mediated by miR-224 in mud crab, the target genes controlled by miR-224 were predicted by Targetscan and miRanda software. The prediction revealed that HSP70 was the potential target gene regulated by miR-224 (Fig. 4A). To ascertain this prediction, synthetic miR-224 and EGFP-HSP70-3'UTR or the mutant EGFP-ΔHSP70-3'UTR were co-transfected into *Drosophila* S2 cells (Fig. 4B). When the EGFP fluorescence activity of these transfectants was observed under a fluorescence microscopy and a microplate reader, a significant decrease in fluorescence intensity was observed in cells co-transfected with EGFP-HSP70-3'UTR compared with control (Figs. 4C and 4D), which indicates that miR-224 potentially interacts with HSP70 to modulate its expression.

To investigate the interaction between miR-224 and HSP70 in mud crabs, miR-224 was silenced or overexpressed followed by HSP70 detection. The results revealed significant increase in both mRNA and protein levels of HSP70 after AMO-miR-224 treatment (Figs. 4E and 4F). On the contrary, the mRNA and protein levels of HSP70 decreased upon miR-224 overexpression (Fig. 4G and 4H). Furthermore, fluorescence *in situ* hybridization (FISH) analysis was carried out to determine the subcellular location of miR-224 and HSP70 in mud crabs hemocytes. When miR-224 and HSP70 mRNA were labeled with fluorescent probes before being observed under a fluorescence microscope, both miR-224 and HSP70 mRNA were found to co-localize

in hemocytes of the mud crabs (Fig. 4I). All these results suggest that HSP70 is the direct target gene of miR-224 in the mud crabs.

Effect of HSP70 on the modulation of hemolymph microbiota homeostasis

To ascertain whether HSP70 is involved in the modulation of miR-224-mediated hemolymph microbiota homeostasis, miR-224-depleted mud crabs were injected with HSP70-siRNA before being infected with *V. parahaemolyticus* and the levels of ALFs and ROS were detected in hemocytes. The results revealed significant increase in the expression of ALF1, ALF4 and ALF5 in the HSP70-siRNA treated group compared with controls (Fig. 5A). Similar results were obtained for ROS levels (Figs. 5B and 5C). Moreover, the expression of HSP70 was significantly decreased in exosome-Vp treated mud crabs as compared with control (Fig. 5D), which indicates that HSP70 participates in exosome-mediated regulatory process. Besides, in HSP70-depleted mud crabs co-injected with *V. parahaemolyticus* and exosome-PBS, there were lower hemolymph bacteria numbers but higher hemolymph bacteria diversity (Figs. 5E and 5F), which suggest that exosome-PBS could also maintain hemolymph microbiota homeostasis when the expression of HSP70 is suppressed. These results suggest that exosomal miR-224 contributes to hemolymph microbiota homeostasis by targeting HSP70 in mud crabs.

Formation of the TRAF6-Ecsit complex in the exosomal regulatory pathway

Based on the observation that HSP70 was relevant in the modulation of hemolymph microbiota homeostasis, pull-down analysis was carried out followed by SDS-PAGE and Western blot analyses. The results showed that HSP70 could bind to TRAF6 (Figs. 6A and 6B). The role of TRAF6 in exosomal miR-224-mediated regulatory process was investigated by silencing the expression of TRAF6 in mud crabs and the expression of ALFs detected by qPCR analysis. As shown in Fig. 6C, the

261 expression levels of ALF1, ALF4 and ALF5 were significantly decreased. Similarly,
262 there was significant decrease in ROS level in hemocytes of TRAF6-silenced mud crabs
263 compared with control (Figs. 6D and 6E). Intriguingly, these data are in contrary to the
264 known function of HSP70 and indicate that HSP70-TRAF6 complex is not the final
265 effector for exosome-mediated hemolymph microbiota homeostasis. Therefore, we
266 performed pull-down analysis based on TRAF6, it was found that TRAF6 could bind
267 with Ecsit (Figs. 6F and 6G). Given that HSP70 could bind to TRAF6, while TRAF6
268 also binds to Ecsit, we went on to use co-immunoprecipitation analysis to determine
269 whether HSP70 could also directly bind to Ecsit. The results showed that HSP70 could
270 not bind to Ecsit (Fig. 6H), which suggests that TRAF6 formed separate complexes
271 with HSP70 and Ecsit. Furthermore, we found that exosome-Vp treatment in the mud
272 crabs suppressed the binding of TRAF6 to HSP70, but enhanced the interaction
273 between TRAF6 and Ecsit compared with exosome-PBS treatment (Fig. 6I). All the
274 above results in this section suggest that during the exosome-mediated regulatory
275 process, interaction between HSP70 and TRAF6 is suppressed, so that the released
276 TRAF6 could form a complex with Ecsit.

277 **Role of the TRAF6-Ecsit complex in modulation of hemolymph microbiota**
278 **homeostasis**

279 The TRAF6-Ecsit complex is required for mitochondrial recruitment to
280 phagosomes and is also involved in ROS production during anti-bacterial response
281 (Geng et al., 2015). Thus, when the expression of TRAF6 in the mitochondria of mud
282 crabs treated with exosome-Vp was determined, an increased level of TRAF6 was
283 observed (Fig. 7A). Moreover, mROS level was also significantly increased in
284 hemocytes of exosome-Vp treated mud crabs compared with controls (Figs. 7B and 7C).
285 These results indicate that released TRAF6 translocate to the mitochondria to form a

286 complex with Ecsit, which then mediates mROS production. Ecsit is not only found in
287 the mitochondria, but also in cytoplasm (Qu et al., 2015). Thus, because TRAF6 also
288 serves as an E3 ubiquitin ligase (Zhang et al., 2016), whether the binding of TRAF6 to
289 Ecsit results in the ubiquitination of Ecsit requires further investigation. Based on this,
290 the effect of TRAF6 silencing on Ecsit ubiquitination was determined. As shown in Fig.
291 7D, TRAF6 knockdown resulted in significant decrease in the ubiquitination of Ecsit
292 inhibit, which suggest that TRAF6 was the ubiquitin ligase of Ecsit. Besides, it was
293 found that the ubiquitination of Ecsit was significantly increased when the mud crabs
294 were treated with exosome-Vp (Fig. 7E). It has been reported that ubiquitination is a
295 signal for nuclear translocation (Geetha et al., 2005). For this reason, when the nuclear
296 translocation of Ecsit was determined using Western blot analysis, the results revealed
297 an increased in the protein level of Ecsit in nuclear extracts of hemocytes from mud
298 crabs injected with exosome-Vp (Fig. 7F). Furthermore, the localization of Ecsit was
299 confirmed by immunofluorescence microscopy technique using mouse anti-Ecsit
300 antibody. The results indicated co-staining of Ecsit with DAPI in hemocytes nuclei (Fig.
301 7G).

302 To explore the effect of Ecsit translocation to the nucleus, dual-luciferase reporter
303 assay was carried out in S2 cells. The results showed that the overexpression of Ecsit
304 resulted in significant activation of ALF1, ALF4 and ALF5 transcription (Fig. 7H). The
305 role of the TRAF6-Ecsit complex in the modulation of hemolymph microbiota
306 homeostasis in mud crabs was then explored using 16S rDNA sequencing after
307 knockdown of TRAF6 and Ecsit, respectively. The results revealed that the mediation
308 of hemolymph microbiota homeostasis by exosome-Vp was disrupted upon silencing
309 of TRAF6 or Ecsit (Figs. 7I and 7J), which indicates that the TRAF6-Ecsit complex is
310 required for exosome-mediated hemolymph microbiota homeostasis.

311 Taken together, the findings in this study indicate that during *V. parahaemolyticus*
312 infection, there is more packaging of miR-224 in the mud crab exosomes. This
313 increased uptake of exosomal miR-224 resulted in HSP70 suppression, which causes
314 disruption of the HSP70-TRAF6 complex in recipient hemocytes, thereby releasing
315 TRAF6 to interact with Ecsit in mitochondria to regulate mROS production. TRAF6
316 also mediates Ecsit ubiquitination and nuclear translocation to facilitate the
317 transcription of ALFs, which affect hemolymph microbiota homeostasis in response to
318 pathogens infection (Fig. 8).
319

320 **Discussion**

321 Exosomes are small bioactive membrane-enclosed vesicles derived from the
322 fusion of multivesicular bodies (MVBs) with the plasma membrane that promote
323 intercellular communication (Schorey and Bhatnagar, 2010). There is growing
324 evidence that exosomes are involved in the regulation of pathogen infection and
325 immune response of the host (Sergeeva and VanDerGoot, 2015). For instance,
326 exosomes released from *Mycobacterium avium* (*M. avium*)-infected macrophages
327 contain GPLs (the major cell wall constituent of *M. avium*) that are transferred to
328 uninfected macrophages to stimulate a proinflammatory response dependent on Toll
329 like receptor (TLR) 2, TLR4, and MyD88 (Bhatnagar and Schorey, 2007). Similarly, it
330 has been reported that exosomes released from macrophages infected with
331 *Mycobacterium tuberculosis*, *Salmonella typhimurium* and *Mycobacterium bovis* could
332 stimulate TNF-α and IL-12 production in mice (Bhatnagar et al., 2007). Currently,
333 studies on exosome-bacterial interaction during infections have mainly been carried out
334 in higher organisms. However, the role of exosomes in anti-bacterial immunity in
335 invertebrates has largely not been explored. Moreover, most of these studies are related

to inflammation regulation (Smith et al., 2017), while the involvement of exosomes in anti-bacterial immunity has never been addressed from the perspective of hemolymph microbiota homeostasis particularly in crustacean. In the current study, we found that exosomes released from *V. parahaemolyticus*-infected mud crabs could reduce crab mortality due to bacterial infection by maintaining hemolymph microbiota homeostasis. This is the first time it has been demonstrated that exosomes play a role during anti-bacterial immunity of invertebrates, and also shows the involvement of exosomes mediation in hemolymph microbiota homeostasis during response to pathogens infection.

One of the typical features of exosomes is the packaging of large numbers of nucleic acids, including miRNA, mRNA, mtDNA, piRNA, lncRNA, rRNA, snRNA and tRNA (Boorn et al., 2013). Given that miRNAs are the most abundant RNA species in exosomes, it has been reported that the molecular composition of the miRNA cargo carried by exosomes can be affected by external signals such as oxidative stress and pathogens infection, which reflects the physiological or pathological state of donor cells (Eldh et al., 2010). Our previous study revealed that miR-137 and miR-7847 were less packaged in mud crab exosomes after WSSV challenge, which resulted in the activation of AIF (apoptosis induce factor) and eventually the induction of apoptosis and suppression of viral infection in recipient mud crab hemocytes (Gong et al., 2020). Besides, miR-145, miR-199a, miR-221 and Let-7f that are assembled in exosomes can directly bind to the genomic RNA of HCV (Hepatitis C virus) to inhibit viral replication in umbilical cord mesenchymal stem cells (Qian et al., 2016). In addition, exosomal miR-21 and miR-29a regulate gene expression in HEK293 cells as well as function as ligands that bind with TLRs to activate relevant immune pathways in recipient cells (Fabbri et al., 2012). Due to their diverse regulatory roles, exosomal miRNAs have been

361 shown in most studies to be crucial regulators of host-pathogen interactions, mainly
362 studies involving viral infections (Nahand et al., 2020). Thus far, the role of exosomal
363 miRNAs in bacterial infections still remain unexplored, especially in invertebrates. The
364 current study reveals that during *V. parahaemolyticus* infection in mud crabs, miR-224
365 was more packaged in exosomes, which resulted in the suppression of HSP70, and
366 eventually affected hemolymph microbiota homeostasis by regulating the levels of
367 ROS and ALFs expression to help clear the infection. This observation reveals a novel
368 regulatory mechanism that shows the role of exosomal miRNAs during innate immune
369 response in invertebrates.

370 Most of the miR-224-associated studies have been conducted in human cancer
371 cells, with miR-224 reported to promote the expression of tumor invasion-associated
372 proteins p-PAK4 and MMP-9 by directly targeting HOXD10 (Li et al., 2014). It has
373 also been shown that miR-224 can be packaged into exosomes released by
374 hepatocellular carcinoma to regulate cell proliferation and invasion by targeting glycine
375 *N*-methyltransferase (Cui et al., 2019). While the role of miR-224 in invertebrates had
376 remained elusive, results from this current study reveals that miR-224 could target
377 HSP70 to disrupt the HSP70-TRAF6 complex or its formation. As an evolutionarily
378 conserved protein, HSP70 plays an essential role during the regulation of cell growth,
379 senescence and apoptosis (Mayer and Bukau, 2005). Studies have shown that HSP70
380 could inhibit LPS-induced NF-κB activation by interacting with TRAF6 to prevent its
381 ubiquitination, which eventually suppresses the production of mediators of
382 inflammation (Chen et al., 2006). Similarly, our current data show that HSP70 could
383 bind with TRAF6 to affect its function in mud crab hemocytes, while the release of
384 TRAF6 from disruption of the HSP70-TRAF6 complex allows TRAF6 to complex with
385 Ecsit. The TRAF6-Ecsit complex is required for mitochondrial recruitment to

386 phagosomes, hence, disruption of the TRAF6-Ecsit complex would severely dampen
387 ROS production and therefore increase susceptibility to bacterial infection (Geng et al.,
388 2015). Both TRAF6 and Ecsit have also been reported to regulate the expression of
389 AMPs during bacterial infection in marine crustaceans (Ding et al., 2014; Wei et al.,
390 2018). In the present study, it was observed that TRAF6 cooperates with Ecsit to
391 regulate mROS and the expression of ALFs in mitochondria and nuclei, respectively,
392 which further affects hemolymph microbiota homeostasis in response to bacterial
393 infection in mud crabs. The present study therefore provides novel insights into how
394 invertebrates mount resistance to pathogenic microbial infections.
395
396 **Materials and Methods**
397 **Ethics statement**
398 The mud crabs used in this study were purchased from a local crab farm
399 (Niutianyang, Shantou, Guangdong, China), and processed according to the
400 Regulations for the Administration of Affairs Concerning Experimental Animals
401 established by the Guangdong Provincial Department of Science and Technology on
402 the Use and Care of Animals. The relevant studies did not involve endangered or
403 protected species and therefore no specific permits were required for the described field
404 studies.
405 **Mud crab culture and *Vibrio parahaemolyticus* challenge**
406 Healthy mud crabs, approximately 50 g each, were acclimated to laboratory
407 conditions in water with 8‰ salinity at 25 ºC for a week before further processed. For
408 pathogen challenge, 200 μL *V. parahaemolyticus* (1×10^7 *cfu*/mL) was injected into the
409 base of the fourth leg of each crab, 10 mM PBS (PH=7.4) was used as control. At
410 different time post-infection, hemolymph was collected from three randomly chosen

411 crabs per group for further investigation (Zhang et al., 2018).

412 **Isolation and analysis of exosomes**

413 For exosomes isolation, 50 mL hemolymph from mud crabs were separated, after
414 centrifuged at 300 × *g* for 5 min, to collect the supernatant. Next, supernatants were
415 subjected to ultracentrifugation, followed by sucrose density-gradient centrifugation
416 and filtrated through filters (pore size of 0.22 μm). The obtained exosomes were
417 observed by Philips CM120 BioTwin transmission electron microscope (FEI Company,
418 USA), while the quantity and size of the exosomes were measured by Nano-Sight
419 NS300 (Malvern Instruments Ltd, UK).

420 **Microarray analysis of exosomal miRNAs**

421 Exosomal miRNA microarray analysis was performed at Biomarker Technologies
422 (Beijing, China), using Agilent Human miRNA 8*60 K V21.0 microarray (Agilent
423 Technologies, USA). The NCBI BioProject database accession number is
424 PRJNA600674. Quantile normalization and data processing were carried out using
425 Gene Spring Software 12.6 (Agilent Technologies), hierarchical clustering analysis of
426 the differential expressed miRNAs was conducted by Cluster 3.0 and TreeView
427 software.

428 **Prediction of target genes**

429 The target genes of miR-224 were predicted by a commercial company
430 (BioMarker, Beijing, China) using Targetscan and miRanda software
431 (http://www.targetscan.org; http://www.microrna.org/). The overlapped target genes
432 predicted by the two algorithms were served as the candidate target gene.

433 **Overexpression and silencing of miR-224 in mud crabs**

434 The miRNA mimics and anti-microRNA oligonucleotides (AMOs) of miR-224
435 were injected at 30 μg/crab for 48 h to overexpress and knockdown miR-224 in mud

crab respectively. miR-224 mimic (5'-AGAGACAAGTGAC**A**AA**C**A-3') and AMO-miR-224 (5'-TGTTTGTCACTTG**T**CT**C**T-3') were modified with 2'-*O*-methyl (OME) (bold letters) and the remaining nucleotides phosphorothioated. All oligonucleotides were synthesized by Sangon Biotech (Shanghai, China).

Cell culture, transfection, and fluorescence assays

The *Drosophila* Schneider 2 (S2) cells were cultured at 27 ºC with Express Five serum-free medium (SFM) (Invitrogen, USA). The EGFP-HSP70-3'UTR or mutant plasmids (100 ng/well) and the synthesized miR-224 (50 nM/well) were co-transfected into S2 cells using Cellfectin II Reagent (Invitrogen, USA) according to the manufacturer's protocol. At 48 h post-transfection, the EGFP fluorescence in S2 cells were observed under an inverted fluorescence microscope (Leica, Germany) and measured by a Flex Station II microplate reader (Molecular Devices, USA) at 490/ 510 nm of excitation/emission (Ex/Em).

RNA interference assay

Based on the nucleotide sequence of HSP70, TRAF6 and Ecsit, the specific siRNAs targeting these genes were designed, i.e., HSP70-siRNA (5'-UCUUCAUAAGCACCAUAGAGGAGUU-3'), TRAF6-siRNA (5'-GCUUCUCCCA GCUUGCAAUUU-3') and Ecsit-siRNA (5'-CCCUGUACUCUUCACACAAUU-3'). The siRNAs were synthesized using *in vitro* Transcription T7 Kit (TaKaRa, Dalian, China) according to the manufacturer's instructions. Next, 50 μg of each siRNA was injected into each mud crab. At different time points post injection, three mud crabs were randomly selected for each treatment and stored for later use.

Quantitative real-time PCR

Quantitative real-time PCR was conducted to quantify the mRNA levels using Premix Ex Taq (Takara, Japan). Total RNA was extracted from mud crab hemocytes,

followed by first-strand cDNA synthesis using PrimeScript™ RT Reagent Kit (Takara, Japan). Primers ALF1-F (5'-AACTCATCACGGAGAATAACGC-3'), ALF1-R (5'-CTTCCTCGTTGTTTTCACCCTC-3'); ALF2-F (5'-TGTCGCTCAGGGACTCATC AC-3'), ALF2-R (5'-GGAGATCACGGGAGAGTGAATG-3'); ALF3-F (5'- GAACG GACTCATCACACAGCAG-3'), ALF3-R (5'-CACTTCCTTGTTCTCTTCGCTC-3'); ALF4-F (5'-CACTACTGTGTCCTGAGCCGC-3'), ALF4-R (5'- GTCCTCGCCTTA CAATCTTCTG-3'); ALF5-F (5'-CTTGAAGGGACGAGGTGATGAG-3'), ALF5-R (5'-TGACCAGCCCATTCGCTACAG-3'); ALF6-F (5'-ACAGGGCTATCGCAGAC TTCG-3'), ALF6-R (5'-GCACCTCTTTGGCACACTATTTG-3') were used to quantify transcripts levels of ALFs. Relative fold change were determined using the $2^{-\Delta\Delta Ct}$ algorithm (Arocho et al., 2006).

Hemolymph bacteria counting and sequencing

5 mL mud crab hemolymph were collected after specific treatments and then stained with SYBR®Green I solution (1:40 v/v SYBR®Green I in 1× Tris EDTA buffer). Next, the bacteria number were counted under 100× magnification using a fluorescence microscope (Axio Imager M2, Zeiss, Germany) (Zhang et al., 2018). For 16S rDNA genes sequencing, the total genome DNA of hemolymph microbiota was extracted using QIAamp® PowerFecal® DNA Kit (Qiagen, Germany). All samples were sequenced on Illumina Nova platform by a commercial company (Novogene, Beijing, China) by amplifying the V4 region of the 16S rDNA gene, the data were uploaded to NCBI BioProject database (accession number PRJNA669103).

Cellular and mitochondrial ROS measurement

5 mL hemolymph from three randomly chosen mud crabs per group were drawn into tubes containing ACD anticoagulant buffer, and then centrifuged immediately at 800 ×*g* for 20 min at 4 ℃ to isolate the hemocytes. Next, flow cytometry method was

used to measure cellular ROS level with a ROS Assay Kit (Beyotime Biotechnology, China). For mitochondrial ROS measurement, the ROS intensity was analyzed by MitoSOX Red Mitochondrial Superoxide Indicator (Invitrogen, USA). The fluorescence in hemocytes was observed using an inverted fluorescence microscope (Leica, Germany) and measured by a Flex Station II microplate reader (Molecular Devices, USA).

Statistical analysis

All data were subjected to one-way ANOVA analysis using Origin Pro8.0, with $P < 0.01$ considered as statistically significant. All experiments were carried out in triplicates and repeated for three biological replicates.

Acknowledgments

This study was financially supported by Key Special Project for Introduced Talents Team of Southern Marine Science and Engineering Guangdong Laboratory (Guangzhou) (GML2019ZD0606), National Natural Science Foundation of China (31802341, 42076125, 41876152), Natural Science Foundation of Guangdong Province, China (2018A030307044) and Guangdong Provincial Special Fund for Modern Agriculture Industry Technology Innovation Teams (2019KJ141). The funders had no role in study design, data collection and analysis, decision to publish, or preparation of the manuscript.

Author contributions

YG, XYW, WWS, XR and JC performed the experiments, YG and SKL designed the experiments and analysed the data, HYM and YLZ provided technical supports, YG, JJA, KGC and SKL wrote the manuscript. All authors read and approved the contents of the manuscript and its publication.

Conflict of interest

The authors declare no conflicts of interest.

References

Ambros, V. (2004). The functions of animal microRNAs. Nature *431*, 350-355.

Arocho, A., Chen, B.Y., Ladanyi, M., and Pan, Q.L. (2006). Validation of the 2(-Delta Delta Ct) calculation as an alternate method of data analysis for quantitative PCR of BCR-ABL P210 transcripts. Diagn Mol Pathol *15*, 56-61.

Bang, C., Batkai, S., Dangwal, S., Gupta, S.K., Foinquinos, A., Holzmann, A., Just, A., Remke, J., Zimmer, K., and Zeug, A. (2014) Cardiac fibroblast–derived microRNA passenger strand-enriched exosomes mediate cardiomyocyte hypertrophy. J Clin Invest *124*, 2136-2146.

Bhatnagar, S., and Schorey, J.S. (2007). Exosomes released from infected macrophages contain mycobacterium avium glycopeptidolipids and are proinflammatory. J Biol Chem *282*, 25779-25789.

Bhatnagar, S., Shinagawa, K., Castellino, F.J., and Schorey, J.S. (2007). Exosomes released from macrophages infected with intracellular pathogens stimulate a proinflammatory response in vitro and in vivo. Blood *110*, 3234-3244.

Bobrie, A., Colombo, M., Krumeich, S., Raposo, G.A., and Théry, C. (2012). Diverse subpopulations of vesicles secreted by different intracellular mechanisms are present in exosome preparations obtained by differential ultracentrifugation. J Extracell Vesicles *1*, 18397.

Boorn, J.G.V.D., Daler, J., Coch, C., Schlee, M., and Hartmann, G. (2013). Exosomes as nucleic acid nanocarriers. Adv Drug Deliv Rev *65*, 331-335.

Chen, H., Wu, Y., Zhang, Y., Jin, L., Luo, L., Xue, B., Lu, C., Zhang, X., and Yin, Z. (2006). Hsp70 inhibits lipopolysaccharide-induced NF-kappaB activation by interacting with TRAF6 and inhibiting its ubiquitination. FEBS Lett *580*, 3145-3152.

Colombo, M., Raposo, G.A., and Théry, C. (2014). Biogenesis, secretion, and

intercellular interactions of exosomes and other extracellular vesicles. Annu Rev Cell Dev Biol *30*, 255-289.

Cui, Y., Xu, H.F., Liu, M.Y., Xu, Y.J., He, J.C., Zhou, Y., and Cang, S.D. (2019). Mechanism of exosomal microRNA-224 in development of hepatocellular carcinoma and its diagnostic and prognostic value. World J Gastroenterol *25*, 1890-1898.

Ding, D., Chen, X.W., Kang, L.H., Jiang, H.S., and Kang, C.J. (2014). Role of evolutionarily conserved signaling intermediate in Toll pathways (ECSIT) in the antibacterial immunity of Marsupenaeus japonicus. Dev Comp Immunol *46*, 246-254.

Douglas, A.E. (2018). What will it take to understand the ecology of symbiotic microorganisms? Environ Microbiol *20*, 1920-1924.

Eldh, M., Ekström, K., Valadi, H., Sjöstrand, M., Olsson, B., Jernås, M., and Lötvall, J. (2010). Exosomes communicate protective messages during oxidative stress; possible role of exosomal shuttle RNA. Plos One *5*, e15353.

Fabbri, M., Paone, A., Calore, F., Galli, R., Gaudio, E., Santhanam, R., Lovat, F., Fadda, P., Mao, C., and Nuovo, G.J. (2012). MicroRNAs bind to Toll-like receptors to induce prometastatic inflammatory response. P Natl Acad Sci USA *109*, 12278-12279.

Florie, D., Patrick, L.C., Benjamin, B., Ivan, L., Benoît, T., Christine, P., and Yannick, F. (2014). Exploring the hologenome concept in marine bivalvia: haemolymph microbiota as a pertinent source of probiotics for aquaculture. FEMS Microbiol Lett *350*, 107-116.

Fong, M.Y., Zhou, W., Liu, L., Alontaga, A.Y., and Wang, S.E. (2015). Breast-cancer-secreted miR-122 reprograms glucose metabolism in premetastatic niche to promote metastasis. Nat Cell Biol *17*, 183-194.

Geetha, T., Kenchappa, R.S., Wooten, M.W., and Carter, B.D. (2005). TRAF6-mediated ubiquitination regulates nuclear translocation of NRIF, the p75

566 receptor interactor. Embo J *24*, 3859-3868.

567 Geng, J., Sun, X., Wang, P., Zhang, S., Wang, X., Wu, H., Hong, L., Xie, C., Li, X.,
568 and Zhao, H. (2015). The kinases Mst1 and Mst2 positively regulate phagocyte ROS
569 induction and bactericidal activity. Nat Immunol *16*, 1142-1152.

570 Gong, Y., Kong, T., Ren, X., Chen, J., and Li, S. (2020). Exosome-mediated apoptosis
571 pathway during WSSV infection in crustacean mud crab. Plos Pathog *16*, e1008366.

572 Gurwitz, D. (2015). Exosomal MicroRNAs in Tissue Crosstalk. Drug Dev Res *76*, 259-
573 262.

574 Hammond, S.M., Bernstein, E., Beach, D., and Hannon, G.J. (2000). An RNA-directed
575 nuclease mediates post-transcriptional gene silencing in Drosophila cells. Nature *404*,
576 293.

577 Li, Q., Ding, C., Chen, C., Zhang, Z., Xiao, H., Xie, F., Lei, L., Chen, Y., Mao, B., and
578 Jiang, M. (2014). miR-224 promotion of cell migration and invasion by targeting
579 Homeobox D 10 gene in human hepatocellular carcinoma. J Gastroenterol Hepatol *29*,
580 835-842.

581 Li, S., Sun, L., Wu, H., Hu, Z., Liu, W., Li, Y., and Wen, X. (2012). The intestinal
582 microbial diversity in mud crab (Scylla paramamosain) as determined by PCR-DGGE
583 and clone library analysis. J Appl Microbiol *113*, 1341-1351.

584 Lokmer, A., and Mathias, W.K. (2015). Hemolymph microbiome of Pacific oysters in
585 response to temperature, temperature stress and infection. ISME J *9*, 670-682.

586 Mario, L.S., Caroline, B., Frédéric, B., Claudio, M., Gregor, D.G. Robert, L., Mark, I.,
587 and Michele, D.P. (2014). Endogenous RNAs modulate microRNA sorting to
588 exosomes and transfer to acceptor cells. Cell Rep *8*, 1432-1446.

589 Marisa, M., and Chioma, O. (2015). Exosomes: implications in HIV-1 pathogenesis.
590 Viruses *7*, 4093-4118.

591 Marta, A., and Maria, A. (2015). Exosome biogenesis, regulation, and function in viral
592 infection. Viruses *7*, 5066-5083.
593 Mayer, M.P., and Bukau, B. (2005). Hsp70 chaperones: cellular functions and
594 molecular mechanism. Cell Mol Life Sci *62*, 670-684.
595 Milane, L., Singh, A., Mattheolabakis, G., Suresh, M., and Amiji, M.M. (2015).
596 Exosome mediated communication within the tumor microenvironment. J Control
597 Release *219*, 278-294.
598 Nahand, J.S., Mahjoubin-Tehran, M., Moghoofei, M., Pourhanifeh, M.H., and Hamblin,
599 M.R. (2020). Exosomal miRNAs: novel players in viral infection. Epigenomics *12*,
600 353-370.
601 Paulina, S., Diego, R.R., Marylise, D., Julien, D.L., Evelyne, B., and Delphine, D.G.
602 (2012). The antimicrobial defense of the Pacific oyster, Crassostrea gigas. How
603 diversity may compensate for scarcity in the regulation of resident/pathogenic
604 microflora. Front Microbiol *3*, 160.
605 Qian, X., Xu, C., Fang, S., Zhao, P., Wang, Y., Liu, H., Yuan, W., and Qi, Z. (2016).
606 Exosomal microRNAs derived from umbilical mesenchymal stem cells inhibit hepatitis
607 C virus infection. Stem Cell Transl Med *5*, 1190-1203.
608 Qu, F.F., Xiang, Z.M., Wang, F.X., Zhang, Y., Li, J., Zhang, Y.H., Xiao, S., and Yu,
609 Z.N. (2015). Identification and function of an evolutionarily conserved signaling
610 intermediate in Toll pathways (ECSIT) from Crassostrea hongkongensis. Dev Comp
611 Immunol *53*, 244-252.
612 Schorey, J.S., and Bhatnagar, S. (2010). Exosome function: from tumor immunology
613 to pathogen biology. Traffic *9*, 871-881.
614 Schroeder, M.R. (2007). Molecular basis for target RNA recognition and cleavage by
615 human RISC. Cell *130*, 101-112.

Sergeeva, O.A., and VanDerGoot, F.G. (2015). Kicking out pathogens in exosomes. Cell *161*, 1241-1242.

Smith, V.L., Cheng, Y., Bryant, B.R., and Schorey, J.S. (2017). Exosomes function in antigen presentation during an in vivo Mycobacterium tuberculosis infection. Sci Rep *7*, 43578.

Söderhäll, I. (2016). Crustacean hematopoiesis. Dev Comp Immunol *58*, 129-141.

Sun, W.W., Zhang, X.X., Wan, W.S., Wang, Q., Wen, X.B., Zheng, H.P., Zhang, Y.L., and Li, S.K. (2017). Tumor necrosis factor receptor-associated factor 6 (TRAF6) participates in anti-lipopolysaccharide factors (ALFs) gene expression in mud crab. Dev Comp Immunol *67*, 361-376.

Tkach, M., and Théry, C. (2016). Communication by extracellular vesicles: where we are and where we need to go. Cell *164*, 1226-1232.

Tubiash, H.S., Sizemore, R.K., and Colwell, R.R. (1975). Bacterial flora of the hemolymph of the Blue crab, Callinectes sapidus: most probable numbers. Appl Environ Microb *29*, 388-392.

Valadi, H., Ekström, K., Bossios, A., Sjöstrand, M., Lee, J.J., and Lötvall, J.O. (2007). Exosome-mediated transfer of mRNAs and microRNAs is a novel mechanism of genetic exchange between cells. Nat Cell Biol *9*, 654-659.

Wang, X.W., Xu, J.D., Zhao, X.F., Vasta, G., R., and Wang, J.X. (2014a). A shrimp C-type lectin inhibits proliferation of the hemolymph microbiota by maintaining the expression of antimicrobial peptides. J Biol Chem *289*, 11779-11790.

Wang, J.J., Chen, C., Xie, P.F., Pan, Y., Tan, Y.H., and Tang, L.J. (2014b). Proteomic analysis and immune properties of exosomes released by macrophages infected with Mycobacterium avium. Microbes Infect *16*, 283-291.

Wang, X.W., and Wang, J.X. (2015). Crustacean hemolymph microbiota: Endemic,

641 tightly controlled, and utilization expectable. Mol Immunol *68*, 404-411.

642 Wei, Z.B., Sun, W.W., Tran, N.T., Gong, Y., Ma, H.Y., Zheng, H.P., Zhang, Y.L., and

643 Li, S.K. (2018). Two novel serine proteases from Scylla paramamosain involved in the

644 synthesis of anti-lipopolysaccharide factors and activation of prophenoloxidase system.

645 Fish Shellfish Immun *84*, 322-332.

646 Zhang, J., Li, S., Li, L., Li, M., Guo, C., Yao, J., and Mi, S. (2015). Exosome and

647 exosomal microRNA: trafficking, sorting, and function. Genomics Proteomics

648 Bioinformatics *13*, 17-24.

649 Zhang, X., Li, C.F., Zhang, L., Wu, C.Y., Han, L., Jin, G., Rezaeian, A.H., Han, F.,

650 Liu, C., and Xu, C. (2016). TRAF6 restricts p53 mitochondrial translocation, apoptosis,

651 and tumor Suppression. Mol Cell *64*, 1-12.

652 Zhang, X.X., Zaiqiao, S., Zhang, X.S., Zhang, M., and Li, S.K. (2018). Hemolymph

653 microbiomes of three aquatic invertebrates as revealed by a new cell extraction method.

654 Appl Environ Microb *84*, e02824-17.

Figure legends

Fig 1. Exosomes secreted from *Vibrio parahaemolyticus*-infected mud crab participate in anti-bacterial regulation. (A-B) Exosomes isolated from mud crabs injected with PBS and *V. parahaemolyticus* were detected by electron microscopy **(A)** and Nanosight particle tracking analysis **(B)**. Scale bar, 200 nm. **(C)** Western blot analysis of exosomal protein markers (Flotillin-1 and TSG101) and cytoplasmic marker Calnexin in cell lysate and exosomes. **(D)** The delivery of exosomes to mud crab hemocytes. The indicated exosomes (Dio-labeled, green) were injected into mud crabs for 6 h, after which hemocytes (DiI-labeled, red) were isolated and analyzed by confocal microscopy. Scale bar, 20 μm. **(E)** Effects of exosomes on mud crab mortality. The specific treatments are shown on the top and the mortality was examined daily. **(F)** Effects of exosomes on bacteria number in mud crab hemolymph. Hemolymph bacteria number for the different treatments were counted using a fluorescence microscope at 100× magnification. (Vp means *V. parahaemolyticus*, exosome-Vp or exosome-PBS means exosomes isolated from the hemolymph of crabs challenged with *V. parahaemolyticus* or PBS). Significant statistical differences between treatments are indicated with asterisks (**, $p<0.01$).

Fig 2. Exosomes regulate hemolymph microbiota homeostasis through activation of ROS and ALFs. (A-B) The effects of the indicated exosomes on ROS production during *V. parahaemolyticus* infection in mud crabs. The level of ROS was measured by fluorescence microscopy, Scale bar, 100 μm **(A)** and microplate reader **(B)**. **(C)** The effect of exosomes on the mRNA levels of ALF1-ALF6 and β-actin, used as internal reference. **(D)** The effects of the indicated exosomes on hemolymph microbiota diversity. Mud crabs were co-injected with exosomes and *V. parahaemolyticus* for 48 h, after which hemolymph was collected and subjected to 16S rDNA sequencing. **(E-**

F) The effects of the indicated exosomes on the composition of hemolymph microbiota at phylum (Top 10) **(E)** and genera (Top 35) **(F)** levels. Data represent mean ± s.d. of triplicate assays (*, $p<0.05$; **, $p<0.01$).

Fig 3. Exosomal miR-224 modulates hemolymph microbiota homeostasis in mud crabs. (A) miRNA microarray analysis for exosome-V.p and exosome-PBS is presented as a heatmap. The top three up- and downregulated miRNAs in the indicated exosomes are listed. **(B-C)** The effects of the indicated miRNAs on ALF1 expression in mud crabs. Mimics **(B)** or AMOs **(C)** of the indicated miRNAs were co-injected with *V. parahaemolyticus* into mud crabs for 48 h, followed by the analysis of ALF1 expression using qPCR. **(D)** The expression levels of miR-224 in mud crabs challenged with different exosomes. **(E-F)** The participation of miR-224 in exosome-mediated ROS production. The indicated exosomes, AMO-miR-224 and *V. parahaemolyticus* were co-injected into mud crabs, followed by the detection of ROS using fluorescence microscopy, Scale bar, 100 μm **(E)** and microplate reader **(F)**. **(G)** The effect of miR-224 silencing on exosome-mediated ALFs regulation. **(H-I)** The involvement of miR-224 in exosome-mediated hemolymph microbiota homeostasis. Hemolymph was collected from mud crabs with the indicated treatments, following by determining the bacterial cell count **(H)** and species **(I)** analysis. Each experiment was performed in triplicate and data are presented as mean ± s.d. (*, $p<0.05$; **, $p<0.01$).

Fig 4. HSP70 is the direct downstream target for miR-224 in mud crab. (A) Target gene prediction of miR-224 using Targetscan and miRanda softwares. **(B)** Cloning of wild-type and mutated 3'UTRs of HSP70 into the pIZ-V5-EGFP plasmid. The sequences targeted by miR-224 are underlined. **(C-D)** The direct interactions between miR-224 and HSP70 in insect cells. *Drosophila* S2 cells were co-transfected with miR-224 and the indicated plasmids for 48 h, followed by analysis of the relative

fluorescence intensities. **(E-F)** The effect of miR-224 silencing on the expression level of HSP70 in mud crab post-injection with AMO-miR-224. The mRNA **(E)** and protein **(F)** levels were examined at 48 h post-injection. **(G-H)** The effect of miR-224 overexpression on the mRNA and protein levels of HSP70 in mud crabs. **(I)** The co-localization of miR-224 and HSP70 mRNA in mud crab hemocytes. The levels of miR-224 and HSP70 mRNA were determined with FAM-labeled miR-224 probe (green) and Cy3-labeled HSP70 mRNA probe (red). Experiments were performed in triplicates, with the data shown representing the mean ± s.d. (**, $p<0.01$).

Fig 5. Role of HSP70 in exosomal miR-224-mediated hemolymph microbiota homeostasis. (A) The participation of HSP70 in miR-224-mediated ALFs regulation in mud crabs. AMO-miR-224 was co-injected with HSP70-siRNA into *V. parahaemolyticus*-challenged mud crabs, followed by analysis of the expression levels of ALFs using qPCR. **(B-C)** The involvement of HSP70 in miR-224-mediated ROS production. The level of ROS in mud crab hemocytes was determined using fluorescence microscopy, Scale bar, 100 μm **(B)** and microplate reader **(C)**. **(D)** The effect of the indicated exosomes on HSP70 expression. Isolated exosomes from mud crabs treated with PBS and *V. parahaemolyticus* were injected into mud crabs, followed by determination of HSP70 protein level using Western blot analysis. **(E-F)** The effect of HSP70 silencing on exosome-mediated hemolymph microbiota homeostasis. Hemolymph was collected from mud crabs with the indicated treatments, and the bacterial cell count **(E)** and species **(F)** analyzed. All the data are the average from at least three independent experiments, mean ± s.d. (*, $p<0.05$; **, $p<0.01$).

Fig 6. miR-224-mediated suppression of HSP70 results in disruption of the HSP70-TRAF6 complex and TRAF6-Ecsit complex formation. (A) Identification of proteins that bind to HSP70. Mud crab hemocytes lysates were subjected to Co-

731 immunoprecipitation (Co-IP) assay using anti-HSP70 IgG, followed by separation
732 using SDS-PAGE and identification of the proteins by mass spectrometry. **(B)**
733 Interactions between HSP70 and TRAF6 in mud crab cell lysates analyzed using Co-
734 IP with anti-HSP70 IgG followed by Western blot analysis. **(C)** The effect of TRAF6
735 silencing on ALFs regulation. Mud crabs were injected with TRAF6-siRNA or GFP-
736 siRNA for 48 h, followed by analysis of ALFs expression using qPCR. **(D-E)** Effect of
737 TRAF6 silencing on ROS production in mud crabs. The level of ROS in mud crab
738 hemocytes was analyzed using fluorescence microscopy, Scale bar, 100 μm **(D)** and
739 microplate reader **(E)**. **(F)** Identification of proteins that bind to TRAF6. The identified
740 proteins are indicated with an arrow. **(G)** The interaction between TRAF6 and Ecsit in
741 mud crabs. **(H)** The interaction between HSP70 and Ecsit in mud crabs. Cell lysates
742 were subjected to Co-IP analysis with anti-HSP70 IgG and anti-Ecsit IgG, followed by
743 Western blot analysis using the indicated antibodies. **(I)** The interactions between
744 HSP70 and TRAF6, TRAF6 and Ecsit in mud crabs after the indicated treatments. Data
745 shown represent the mean ± s.d. for triplicate assays (**, p<0.01).

746 **Fig 7. TRAF6-Ecsit complex mediates hemolymph microbiota homeostasis. (A)**
747 The effect of the indicated exosomes on the protein level of TRAF6 in mitochondria.
748 **(B-C)** The effect of the indicated exosomes on mROS production. The mROS level in
749 mud crab hemocytes was determined using fluorescence microscopy, Scale bar, 50 μm
750 **(B)** and microplate reader **(C)**. **(D)** The effect of TRAF6 silencing on the expression
751 and ubiquitination levels of Ecsit. **(E)** The effect of the indicated exosomes on the
752 expression and ubiquitination levels of Ecsit. **(F)** The protein level of Ecsit in mud crab
753 hemocytes nuclei after treatment with the indicated exosomes was determined by
754 Western blot analysis. Tubulin and Histone H3 were used to evaluate the purity of the
755 isolated nuclei. **(G)** The localization of Ecsit in mud crab hemocytes after treated with

the indicated exosomes was determined using immunofluorescence assay with mouse anti-Ecsit antibody, Scale bar, 10 μm. **(H)** The effect of Ecsit overexpression on the transcription of ALFs. **(I-J)** The effects of TRAF6 or Ecsit silencing on exosome-mediated hemolymph microbiota homeostasis. Hemolymph was collected from mud crabs after the indicated treatments and was used to determine bacteria number **(I)** and species **(J)**. Data shown represent that of three independent experiments (*, $p<0.05$; **, $p<0.01$).

Fig 8. Proposed schematic diagram for exosomal miR-224-mediated hemolymph microbiota homeostasis during *V. parahaemolyticus* infection in mud crabs.

Fig. 1

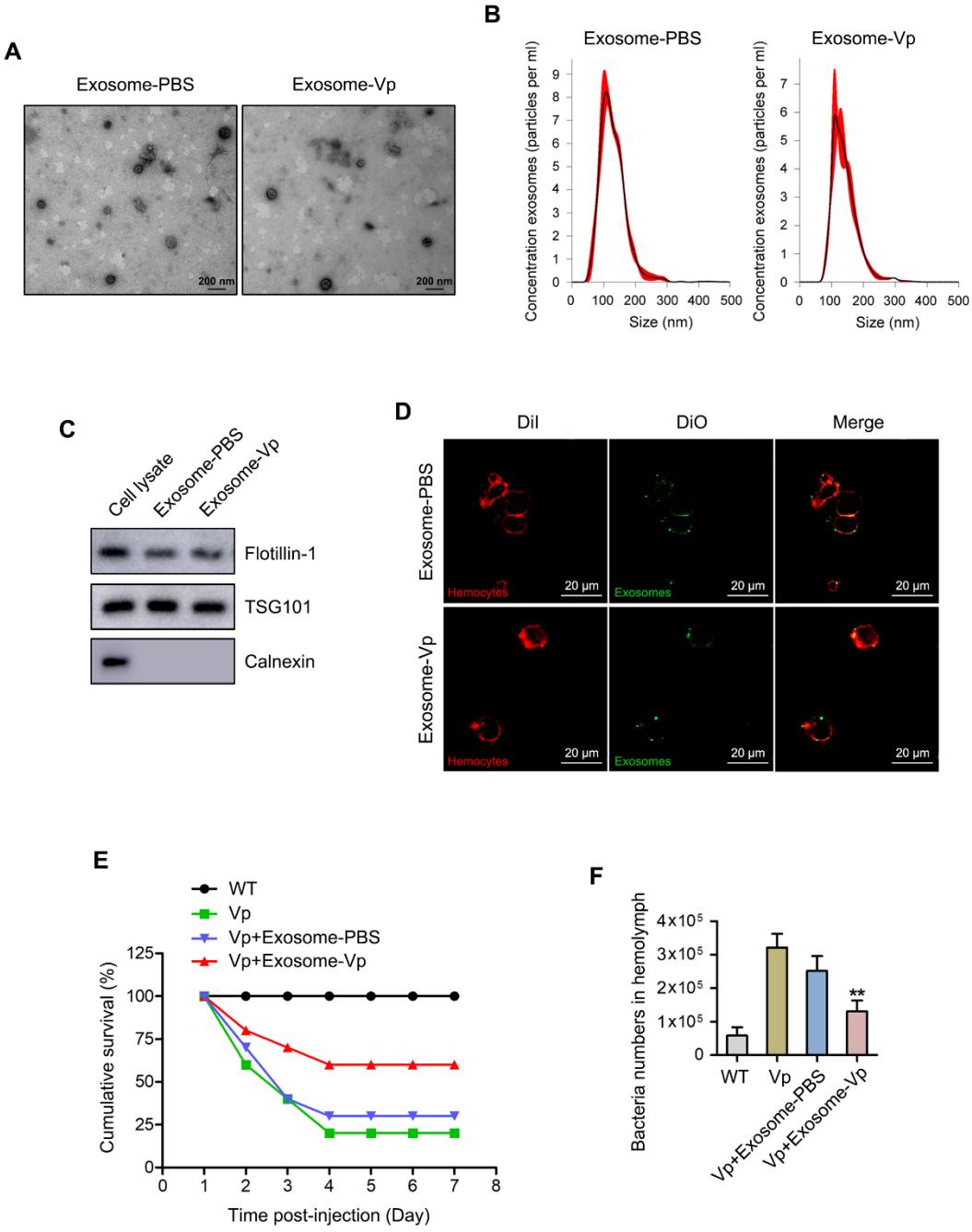

Fig. 2

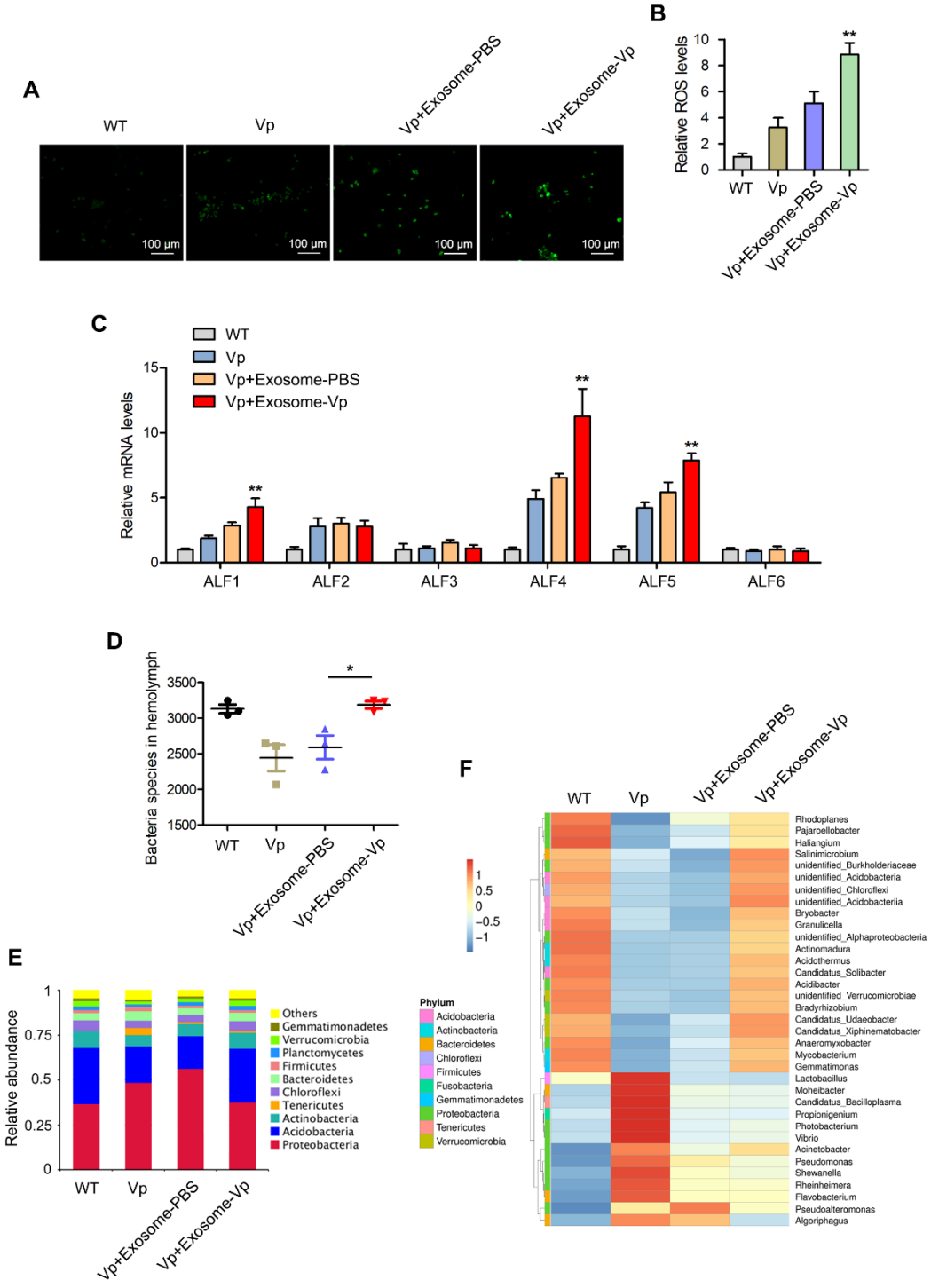

Fig. 3

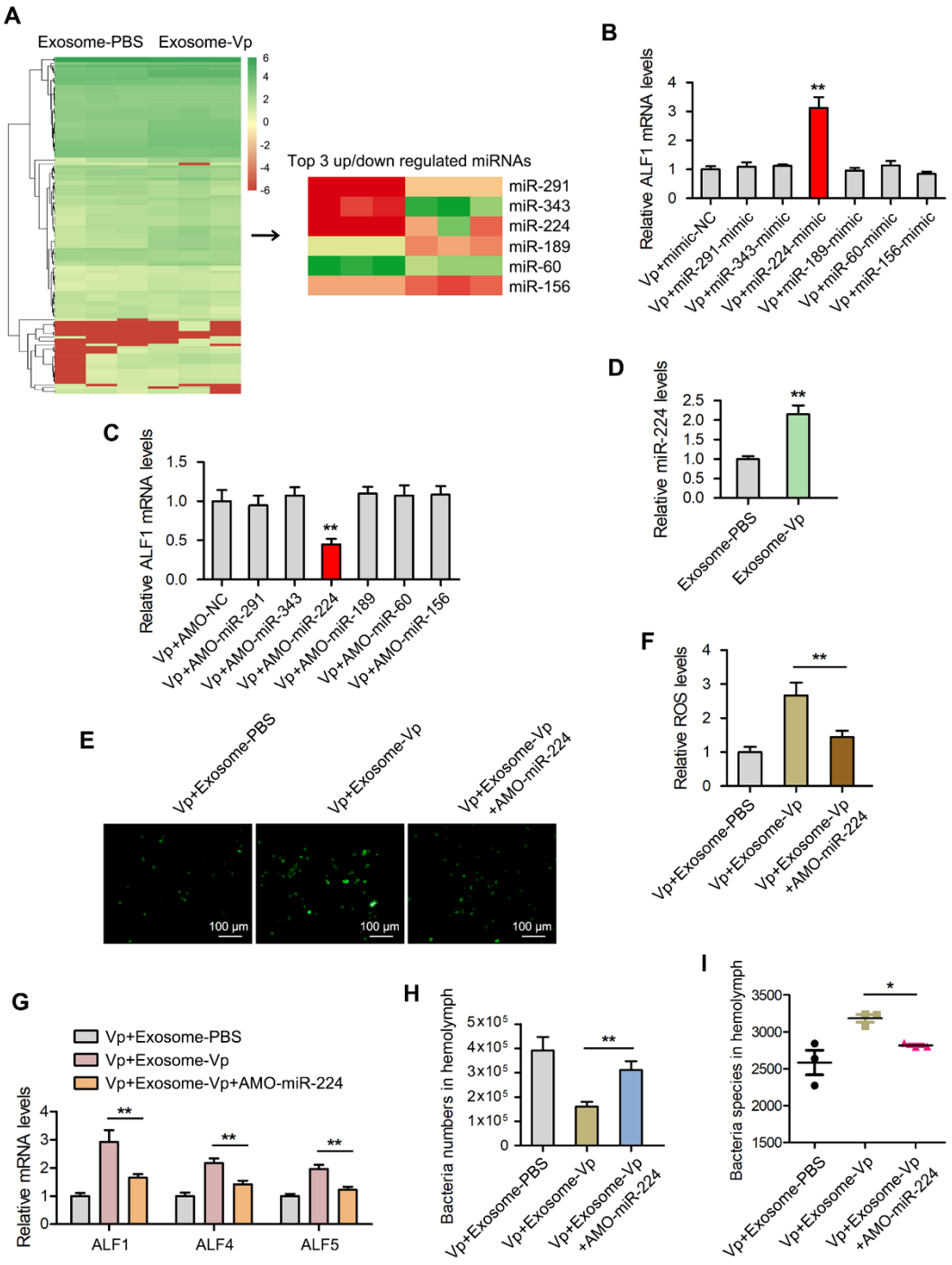

Fig. 4

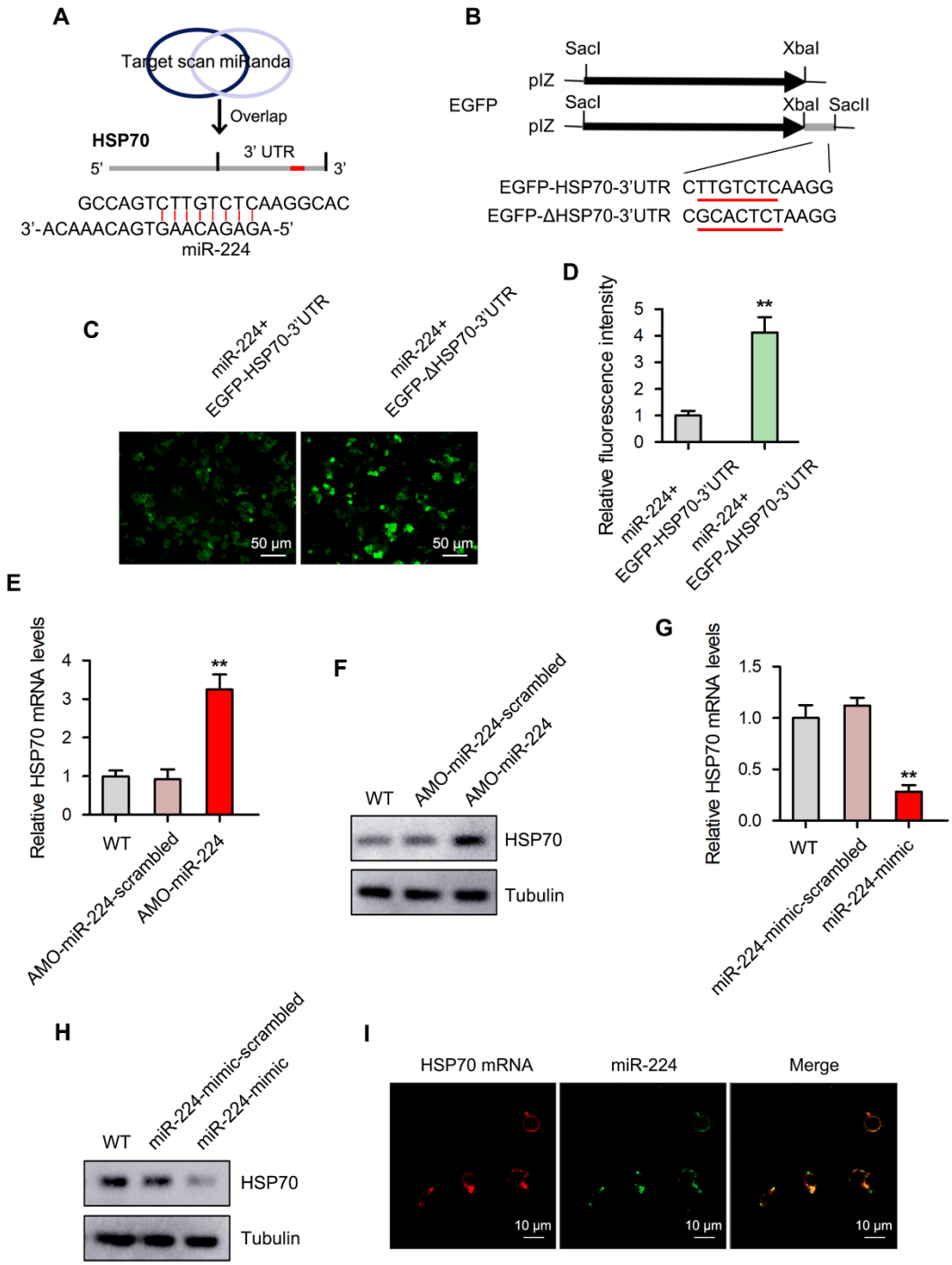

Fig. 5

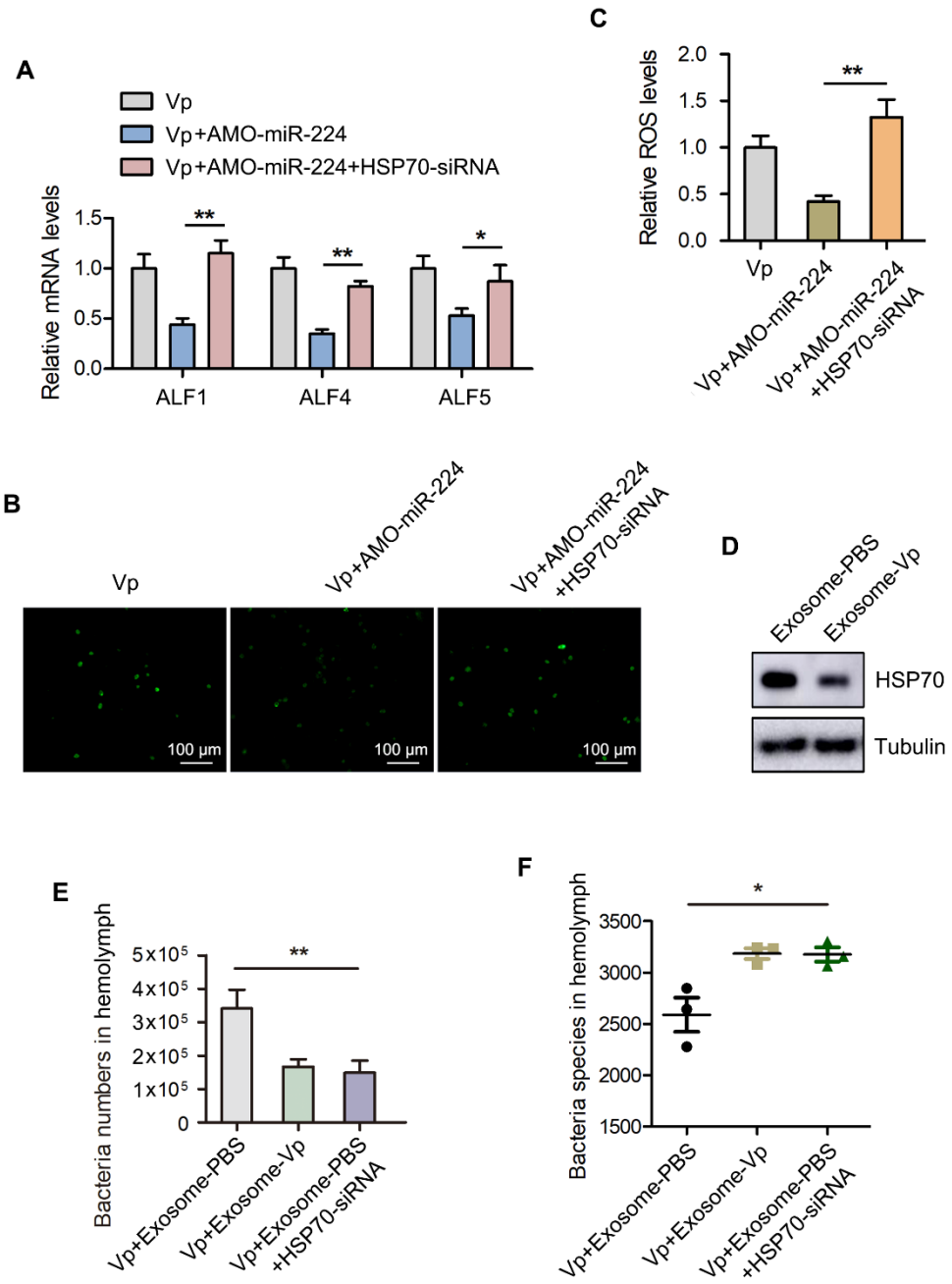

Fig. 6

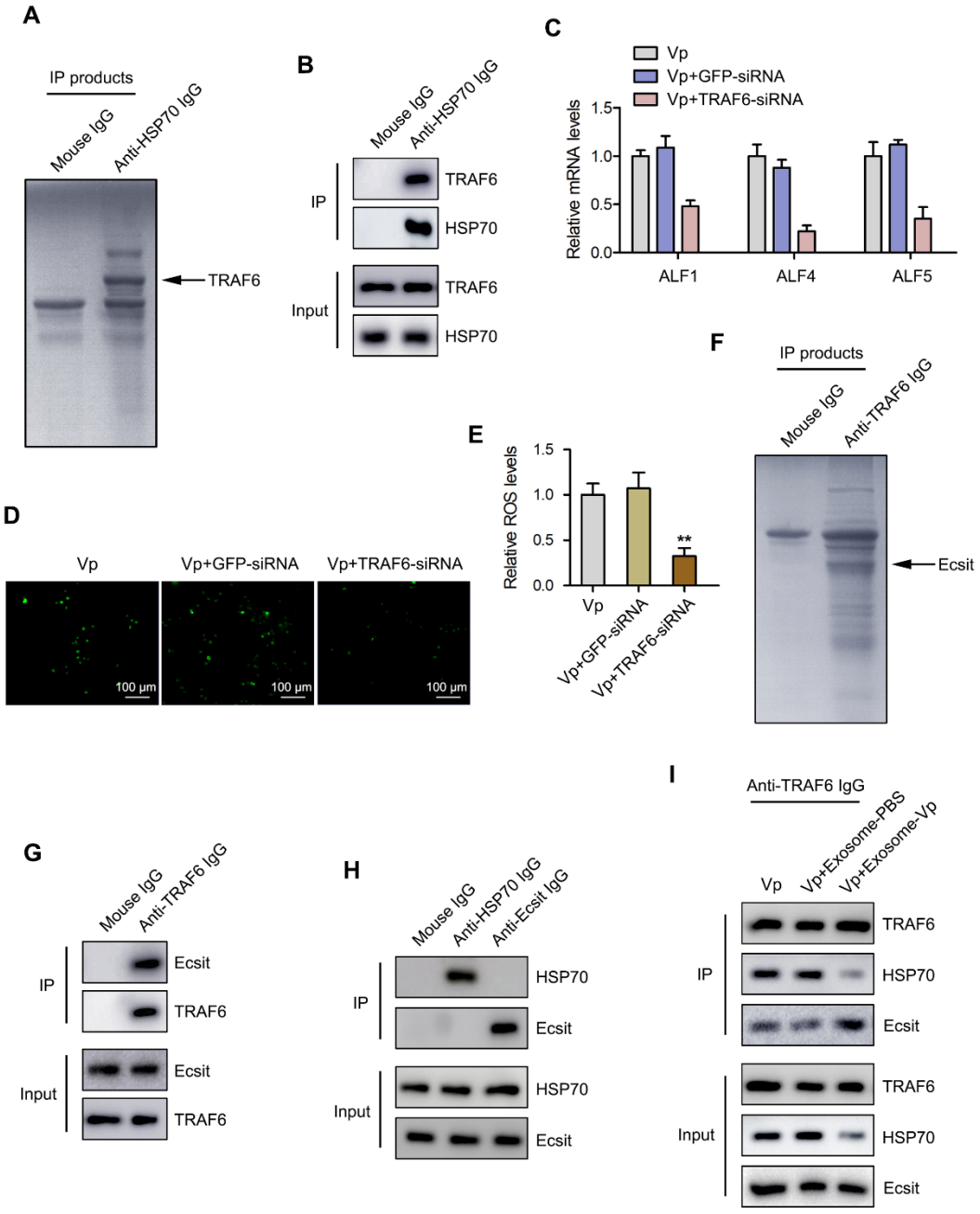

Fig. 7

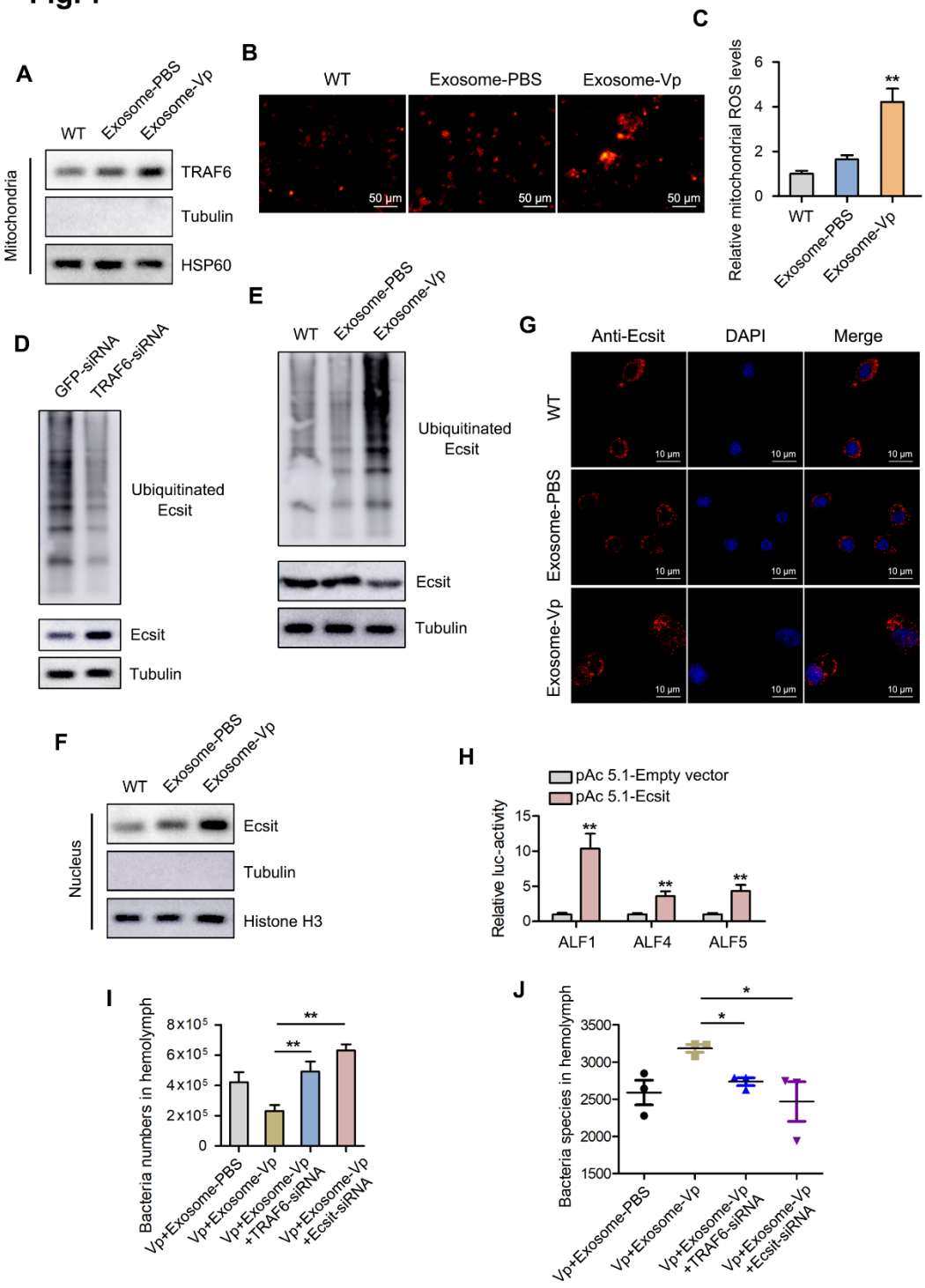

Fig. 8

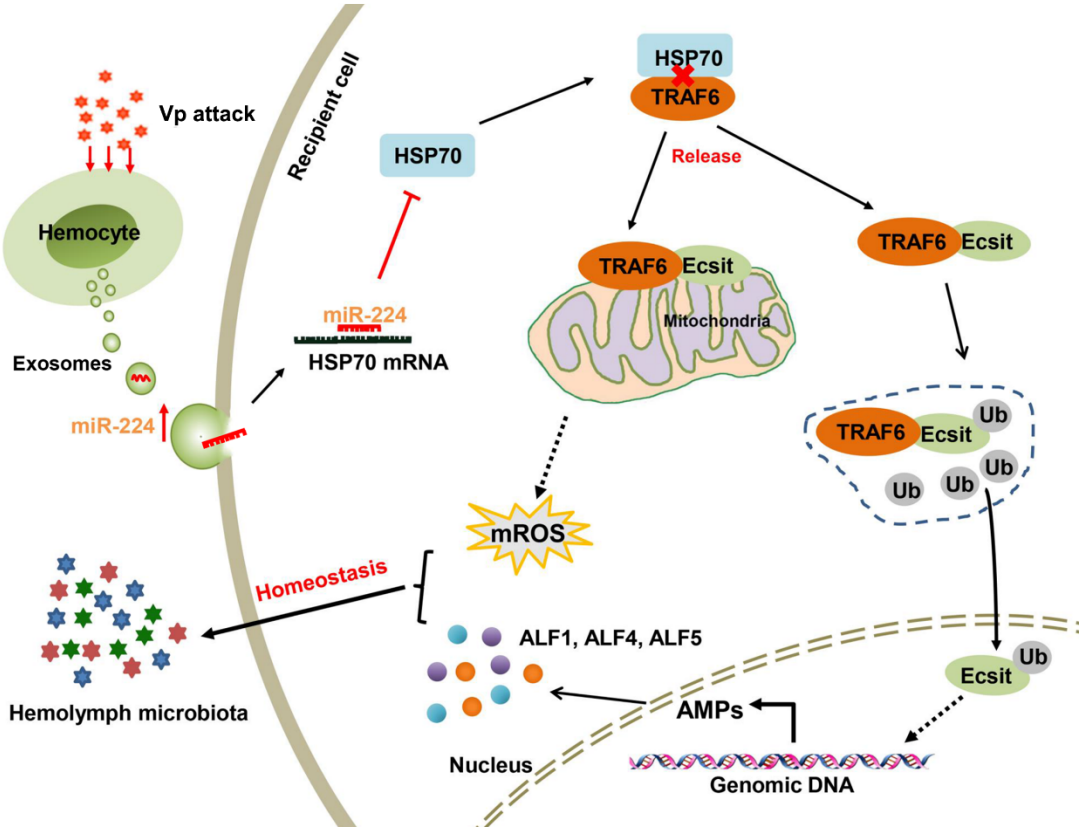

772